Progress in Natural Science: Materials International 27 (2017) 283–288

HOSTED BY

Contents lists available at ScienceDirect

Progress in Natural Science: Materials International

journal homepage: www.elsevier.com/locate/pnsmi

Original Research

Periodic continuum solvation model integrated with first-principles calculations for solid surfaces

Wenjin Yin[a,b], Matthias Krack[c], Xibo Li[b], Lizhen Chen[b], Limin Liu[b,*]

[a] School of Physics and Electronic Science, Hunan University of Science and Technology, Xiangtan 411201, China
[b] Beijing Computational Science Research Center, Beijing 100084, China
[c] Paul Scherrer Institut, CH-5232 Villigen-PSI, Switzerland

ARTICLE INFO

Keywords:
First-principles
Water-solid interface

ABSTRACT

The structural and reactivity properties of the solute in aqueous solution are vital in chemistry and condensed matter physics. In order to understand the detailed adsorption structures and reaction processes on the solid surfaces or liquid/solid interfaces, the solvation effect should be considered in the realistic first-principle calculation. In this work, a periodic continuum solvation model (PCSM) was implemented into a mixed Gaussian and plane-wave density functional theory (DFT) program, CP2K/Quickstep. The reliability of such approach is carefully examined for several typical systems. The results exhibit that the current application can give the accurate solvation energy and reaction pathway for the clusters compared with the available theoretical and experimental ones. We further extend the application to water adsorption on the periodic slab systems, such as metal and semiconductor surface systems. The results reveal that both the adsorption structures and reaction processes are significantly affected by the solvation effect.

1. Introduction

The importance of structural and reactivity properties of the solute in aqueous solution is self-evident. Most of chemical reactions occur in water or other solvents, no matter in nature or the laboratory [1–4]. This is exactly true for biochemistry, most of the organic, inorganic, catalytic chemistry, and a vast part of materials and surface science [1]. On the experimental side, the aqueous solution environment can be easily regulated [5]. On the theoretical side, the general approach is to use explicit water molecules to simulate the aqueous solution environment [6]. However, if all solvent molecules are considered in the simulations, the computational system is usually quite large. Thus the computational cost is extremely high, especially for the first-principle molecular dynamics (FPMD) simulation. Even if the computational cost is feasible for some cases, the structural properties may also vary with the number of the solvent molecules.

In order to save the computational time, the way is to examine the adsorption or the reaction in the vacuum, ignoring the water environment. While the structural and reactivity behaviors of the solute molecules in aqueous solution is rather complex, the accuracy of such calculation may be greatly affected without considering the solvent effect. In order to accurately describe the structural and reactivity properties of the solute in aqueous solution, considerable theoretical works have been done to resolve this problem to resort the continuum solvation model. The general approach is to represent the solvent molecules as a continuous homogeneous and isotropic medium characterized by the dielectric permittivity [2,7–10].

The earliest continuum solvation model was proposed by Onsager, handling the solute molecule by using a sphere cavity [11]. The two most widely used classes of solvation models are the polarizable continuum model (PCM) suggested by Tomasi et al. and the conductor-like screening model (COSMOS) proposed by Klamt and Schuurmann [9,10]. Such techniques have made great successes in the non-periodic system. However, all the models mentioned above are not widely used in condensed matter, not to mention the solid-liquid interfaces.

In order to extend the solvation model to periodic system, Fattebert and Gygi proposed a new independent model [12,13]. The dielectric permittivity in this new model is defined as a smooth self-consistent function of the electronic density of the solute, and placed into the rigorous framework of density functional theory (DFT) [12,14]. This approach was further extended to involve the calculation of cavitation energy by Scherlis et al. [15–17] Following these, the periodic solvation model has been implanted into the DFT program [18]. Marzari et al.

Peer review under responsibility of Chinese Materials Research Society.
* Corresponding author.
E-mail address: limin.liu@csrc.ac.cn (L. Liu).

http://dx.doi.org/10.1016/j.pnsc.2017.03.003
Received 28 May 2015; Accepted 19 June 2016
Available online 30 March 2017

further reformulated to overcome the numerical limitation encountered, which extends its range of applicability in charged species in aqueous solution, along with adding a model for cavitation and dispersion energies [19,20].

Following the approaches of Fattebert and Marzari [12,19], we briefly review the theoretical underpinnings and framework of the periodic continuum solvation model. The implementation of the solvation model derived from DFT in CP2K/Quickstep, a widely used and multi-featured mixed Gaussian and plane-wave DFT code is described [21,22]. Due to the mixed Gaussian and plane wave basis sets, this implementation of the solvation model is suitable for the large periodic slab system. The accuracies of our implementation in CP2K are carefully checked by the solvation energies and reaction energies for both non-periodic and periodic systems, through comparing with the available experimental and theoretical results. The calculated results show that the structural behavior, binding energy, and reactivity are affected by the solvation effect. Therefore, the implanted solvation model is efficient and accurate to determine the solute molecular properties in aqueous solution.

2. Theoretical framework of periodic continuum solvation model

Starting from the basic equations of Fattebert and Gygi [12], the continuum dielectric permittivity functional in solution is introduced, which defines the dielectric permittivity as a function of the electronic density of the solute as follows,

$$\epsilon(\rho^{elec}) = 1 + \frac{\epsilon_\infty}{2}\left(1 + \frac{1 - (\rho^{elec}/\rho_0)^{2\beta}}{1 + (\rho^{elec}/\rho_0)^{2\beta}}\right) \tag{1}$$

This function asymptotically approaches the dielectric permittivity of the bulk solvent, ϵ_∞, in the regions, where the solute electronic density is low. The solute electronic density is high in the other regions (inside the solute cavity). The two parameters, ρ_0 and β, are the electronic density threshold, which determines the solute cavity size and modulates the smoothness of transition from ϵ_∞ to 1. This smoothness function allows dielectric permittivity to be well defined in the three dimensional meshes used in typical calculations. Nonetheless, the total energy and atomic force are usually difficult to converge when this model is used for the periodic slab system [17].

To extend the solvation effect to periodic slab system, a new dielectric permittivity function using a piecewise definition was proposed as follows [19],

$$\epsilon_{\epsilon_\infty,\rho_{min},\rho_{max}}(\rho^{elec}) = \begin{cases} 1 & \rho^{elec} > \rho_{max} \\ \exp(t(\ln \rho^{elec}))\,\epsilon_\infty & \rho_{min} < \rho^{elec} < \rho_{max} \\ \epsilon_\infty & \rho^{elec} < \rho_{min} \end{cases} \tag{2}$$

Unlike Eq. (1), this dielectric permittivity function introduces a smooth function $t(x)$, which is defined as,

$$t(x) = \frac{\ln \epsilon_\infty}{2\pi}\left[2\pi\frac{(\ln \rho_{max} - x)}{(\ln \rho_{max} - \ln \rho_{min})} - \sin\left(2\pi\frac{(\ln \rho_{max} - x)}{(\ln \rho_{max} - \ln \rho_{min})}\right)\right] \tag{3}$$

This smooth function involves the $t(x)$, which monotonically decreases from $t(\ln \rho_{min}) = \ln \epsilon_\infty$ to $t(\ln \rho_{max}) = 0$. It is important to notice that the proposed dielectric permittivity function does not contain any internal adjustable parameters, but only depends on the dielectric permittivity constant ϵ_∞ and two electronic density thresholds ρ_{min} and ρ_{max}.

Combined with the DFT result, the dielectric permittivity of the whole system can be easily computed by the above dielectric permittivity function. Adopting the readily obtained whole system dielectric permittivity, the total electrostatic potential $\Phi^{tot}(r)$ of the whole system can be solved by the dielectric medium Poisson equation written as,

$$\nabla \cdot \epsilon(\rho^{elec}(r))\nabla\Phi^{tot}(r) = -4\pi\rho^{solute}(r) \tag{4}$$

To solve this equation, the general approach is resorted to the finite difference scheme, such as fourth-order and sixth-order or even higher. The density $\rho^{solute}(r)$ is the total charge density of the solute, containing the electronic density $\rho^{elec}(r)$ and the ionic density $\rho^{ion}(r)$ of the solute.

Due to the low computational and MPI parallel efficiency of the Poisson scheme, a more efficiency method depending on iterative procedure was used to calculate the total electrostatic potential of the system. During the iterative procedure, the Eq. (4) can be evolved to a vacuum-like Poisson equation through the Maxwell equation,

$$\nabla^2\Phi^{tot}(r) = -4\pi\rho^{tot}(r) \tag{5}$$

where $\rho^{tot}(r)$ is the total charge density of the system, containing the solute charge density $\rho^{solute}(r)$ and the polarization charge density $\rho^{pol}(r)$ introduced by the polarization effect.

The detail iteration process can be found in this Ref 19. On the basis of obtained $\rho^{pol}(r)$, the polarization potential $\phi^{pol}(r)$ and solute potential $\phi^{solute}(r)$ can be calculated. Furthermore, the polarization energy E_{el}^{pol} and electrostatic energy of the solute E_{el}^{solute} can also be obtained. Combined with these two energies, the total electrostatic energy of the system can be calculated as follows,

$$E^{el} = E_{el}^{solute} + E_{el}^{pol} = \frac{1}{2}\int \rho^{solute}\phi^{solute}dr + \frac{1}{2}\int \rho^{solute}\phi^{pol}dr \tag{6}$$

Integrated the electrostatic energy into the Kohn-Sham energy of the SCF in the standard DFT framework, a new form Kohn-Sham energy can be obtained as follows,

$$E[\rho] = T[\rho] + \int v(r)\rho(r)dr + E_{xc}[\rho] + E^{el} \tag{7}$$

where the first three term are the standard kinetic energy, interaction energy with an external potential, and exchange and correlation energy.

Except for the electrostatic energy contributions, other effects such as cavitation, and repulsion energy also play significant role in the solvation energy of the continuum solvation model. These non-electrostatic effect is concentrated in the first solvation shell, thus an electrostatic term itself is insufficient to describe solvation of solute. According to the definition of Ben-Naim [23], the main terms of other effects can be expressed as,

$$\Delta G^{sol} = \Delta G^{el} + G^{cav} + G^{rep} + G^{dis} + P\Delta V \tag{8}$$

In the equation, it contains the electrostatic, cavitation, repulsion, and pressure term energy. The electrostatic energy ΔG^{el}=G^{el}-G^o, and G^o=$(E^{tot})_{vacuum}$ is the standard DFT energy of the isolated solute in vacuum, and G^{el} is the analogous quantity computed by Eq. (7) in solution. The cavitation energy is the energy to build into the solution the cavity containing the solute. The repulsion and dispersion terms are the continuum equivalent of the non-bonded short-range interactions generated by the Pauli Exclusion Principle and by vdW interactions. The pressure term takes into account the change in volume of the solvated system. Adopting the cavity surface S and volume V in empirical model proposed by Scherlis [15], the solvation energy of the continuum solvation model can be redefined by

$$\Delta G^{sol} = \Delta G^{el} + (\alpha + \beta)S + \beta V \tag{9}$$

where the two factors α and β are solvent-specific tunable parameters that can be fitted, together with the other parameters in the solvation model.

3. Implementation and application of periodic continuum solvation model

The periodic continuum solvation model discussed above is implemented into the CP2K/Quickstep [21] package, which is within the frame of DFT. CP2K/Quickstep employs a hybrid Gaussian and plane

wave basis set and norm conserving Goedecker-Teter-Hutter (GTH) pseudopotentials [21,22,24]. The CP2K/Quickstep solves the Kohn-Sham equation through self-consistent field (SCF) iterations to find the ground electronic state. In order to include the solvation effect, the local potential of the Kohn-Sham Hamiltonian and the expression for the total energy are modified based on the equation (13) as shown in the above section. During the solvation calculation, a strict polarization SCF is included, namely, the solvation effect is only computed as the accuracy of the polarization SCF calculation reaches a given threshold value τ^{scf} for each DFT electronic SCF iteration step. For each polarization iteration, the gradient of the total potential for the system is computed in reciprocal space via one fast Fourier transform (FFT) and three inverse FFTs. In addition, for the numerical stability, we adopt high order (fifth- and seventh-order) finite differences scheme to compute $\nabla \ln \epsilon(\rho^{elec}(r))$ in real space. The generalized Poisson equation is solved using a pre-conditioned conjugate gradient algorithm in each polarization iteration step. The total number of polarization SCF iterations required in the calculation is related to the tolerance value τ^{scf} imposed on the residuals.

In the following, we firstly examine the reliability and accuracy of our periodic continuum solvation model for the non-periodic systems, through comparing the solvation energies and reaction barrier with other theoretical or experimental results. Then, we extend the application of this model to the periodic systems, such as slab or interface structure.

3.1. Computational setups

All the calculation results are performed within the CP2K/Quickstep code. Core electrons are described with norm-conserving Goedecker, Teter, and Hutter (GTH) pseudopotentials [25], along with the PBE functional [21,26,27]. The wave functions of the valence electrons are expanded in terms of Gaussian functions with molecularly optimized double-zeta polarized basis sets (m-DZVP) [28]. For the auxiliary basis set of plane waves a 500 Ry cut-off is used, which yields total energies converged to at least 0.001 eV per atom, as conformed by calculation with higher cutoff energy. The large system size is applied, since CP2K contains only single Γ point for *k*-point sampling. In order to avoid the interaction between the adjacent images, a vacuum spacing of 15 Å is employed for all the systems. Transition states along the reaction pathways are utilized the Climbing Image Nudged Elastic Band (NEB) method [26]. All atoms in the slab are relaxed until the maximum residual force is less than 0.02 eV/Å.

The interaction behavior for the solute adsorbed on the slab surface in aqueous solution is different from that in the vacuum, which can be characterized by the binding energy defined as [29,30],

$$E_{bind}^{sol} = E_{bind}^{vacuum} + E_{sol} \tag{10}$$

where E_{bind}^{vacuum} is binding energy calculated in the vacuum, which can be calculated as,

$$E_{bind}^{vacuum} = E_{slab-adsorbate}^{vacuum} - E_{slab}^{vacuum} - E_{adsorbate}^{vacuum} \tag{11}$$

where $E_{slab-adsorbate}^{vacuum}$ is the total energy of the slab and the solute, E_{slab}^{vacuum} is the total energy of the slab, and the $E_{adsorbate}^{vacuum}$ is the total energy of the isolated solute calculated in the same box.

The E_{sol} is the solvation energy, which can be calculated as

$$E_{sol} = E_{slab-adsorbate}^{solvation} - E_{slab-adsorbate}^{vacuum} \tag{12}$$

In the equation, $E_{slab-adsorbate}^{solvation}$ is the total energy of the slab and solute in aqueous solution, while $E_{slab-adsorbate}^{vacuum}$ is the total energy in vacuum.

3.2. Reliability and applications

3.2.1. Non-periodic system

For the non-periodic system, some neutral molecules, such as H_2O, NH_3, CH_4, and $C_4H_{10}N_2$ are considered as the solute, and the solvent is aqueous solution. Table 1 lists the calculated results of the solvation energies for these species. As shown in Table 1, the calculated solvation energies in this work agree well with other available theoretical results. For example, an isolated H_2O solvation energy of −0.29 eV is a little larger than the other theoretical calculation of −0.31 eV [31,32]. The solvation energy for other organic solutes also agree with the theoretical simulation results [19]. Compared with the experimental results [31,32], only solvation energy of H_2O and C_4H_8O molecules agree well with the experimental results, while some others are within ± 0.16 eV away from the experimental results. It should be noted that main difference in solvation energy between the experiment and theory comes from the no-polar molecule, thus more care should be taken during dealing with such system with the solvation model.

Table 1
Solvation energies (eV) for molecules solute in water obtained with our method (column 1) compared with the other experimental and theoretical results.

Molecules	E_{PCSM}	E_{expt}	E_{other} (a)
H_2O	**−0.29**	**−0.27**	**−0.31**
NH_3	**−0.33**	**−0.19**	**−0.27**
CH_4	**−0.07**	**0.09**	**−0.05**
$C_4H_{10}N_2$	**−0.15**	**−0.32**	**−0.16**
C_3H_9N	**−0.03**	**−0.15**	**−0.01**
C_4H_8O	**−0.14**	**−0.138**	**−0.138**

Apart from the solvation energy, the reaction pathway and energy barrier are further explored by our model for the non-periodic system. Here, we choose the S_N2 reaction as a model to check the reaction pathway and energy barrier. This reaction is a typical bimolecular reaction, which can occur both in gas and solution phase,

$$Cl^- + CH_3Cl \rightarrow CH_3Cl + Cl^-$$

Fig. 1 shows the pathway and energy profile for this reaction, where the blue and red lines are the pathways for the reaction in the vacuum and solution phase, respectively. The calculated energy profiles exhibit that the energy barrier in solution increases significantly compared to that in gas phase. Considering the solvation effect, the energy barrier changes from 0.21 eV in the gas phase to 0.45 eV in the solvation. The energy barrier obtained by our model agrees well with the result of Fattebert and Gygi about 0.63 eV, and it is also close to the explicit solvent result of 0.82 eV [13,33,34]. Therefore, our solvation model is accurate to study chemical reaction in solution.

3.2.2. Periodic system

In the real chemical catalytic reaction, most of the reactions occur on the surface in the aqueous solution. The structure and reaction

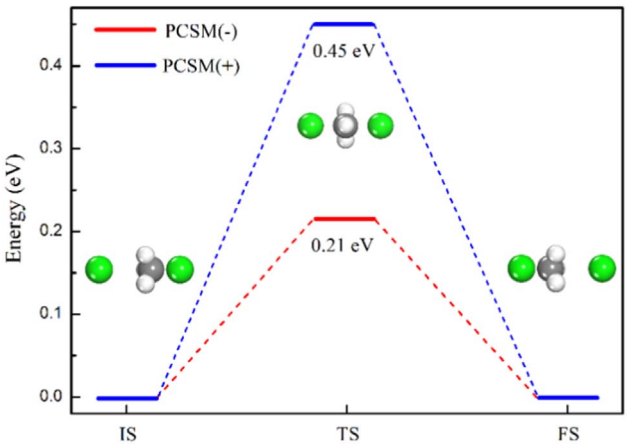

Fig. 1. Energy profile for the reaction pathway of Cl^- + CH_3Cl → CH_3Cl + Cl^- as a function of the distance C-Cl. The Cl, C, and H atom are colored in green, gray, and white, respectively. '-' and '+' mean without and with the solvation effect.

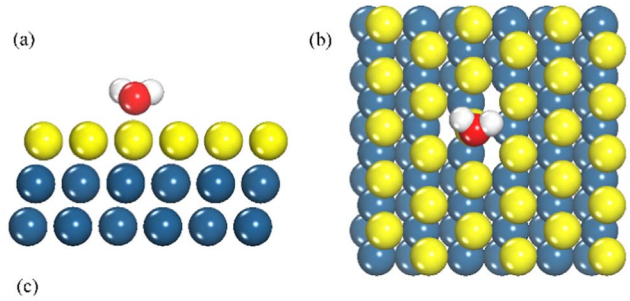

Metal-H_2O	E_{bind} (eV)	E_{bind}[a] (eV)	Pt-O (Å)	O-H (Å)	H-O-H (θ)
PCSM(-)	-0.32	-0.29	2.378	0.98	104.018
PCSM(+)	-0.69	-0.58	2.260	0.978	105.659

Fig. 2. The configuration of a H_2O adsorbed on Pt (111) surface. (a), (b) the side and top view of the H_2O adsorbed on Pt (111) surface, respectively. (c) The binding energies and the relaxed configuration parameters of the H_2O on Pt (111) surface. The O atom in red, H atom in white, and Pt atoms in gray blue except for the top Pt atom layer in yellow.

pathways of the solute on solid surface may be significantly affected by the aqueous solution. Hence, we extend the application of our solvation model to the periodic slab systems.

3.2.2.1. Water adsorption on Pt (111) surface. Here, we firstly consider the system that the H_2O solute adsorbs on metal slab surface in aqueous solution. The platinum (Pt) (111) surface is a typical metal slab surface, which is widely used as catalyst. Here, the water interaction with Pt is considered as a model system to study the solvation effect. The water adsorbs on the Pt (111) slab, containing three Pt atom layers (see Fig. 2).

After geometry optimization, the H_2O molecule almost parallels to the surface of the Pt (111) (see Fig. 2(a)). As shown in Fig. 2(b), the O atom of the H_2O is on the top of the Pt atom, and the H atoms point to the adjacent Pt atoms. The relaxed results of the configuration parameters and binding energies in gas and solution phase are shown in a tabular style in Fig. 2(c). It is obvious that the solvation significantly affects the structural behavior of the solute on the surface. For example, the distance between Pt atom and O atom is 2.378 Å in the vacuum, and it reduces to 2.260 Å as the solvation effect is considered. Meanwhile, the solvation effect changes the angle of the H_2O from 104.02° in vacuum to 105.66°, but has almost no influence on the O-H distance of the H_2O. Besides the solvation effect greatly changes structural properties between the solute and metal surface. The typical binding energy of H_2O on Pt is −0.32 eV in vacuum [35]. When the solvation effect is considered, the binding energy increases to −0.69 eV, which is in consistent with the decreasing tendency of the Pt-O distance. Yao et al. studied the solvation effect on water adsorption on Pt (111) surface, and they found that the binding energy of the H_2O on Pt is −0.58 eV when considering the solvation effect [29]. Thus, our calculated binding energy in solution agrees well with the results of the previous work [29]. In all, the solvation can significantly affect the structural and interaction behavior of the solute interaction with the metal slab system.

3.2.2.2. Water adsorption on the perfect TiO_2 (110) surface. Apart from the metal slab surface, we further explore our solvation model to semiconductor slab surface, which plays vital roles in the photocatalytic splitting water. Among various photo-catalytic semiconductors, TiO_2 is one of the most promising catalysts for water splitting [3]. One long debated question is whether the water is automatically dissociated on the perfect rutile TiO_2 (110) surface during the photocatalysis [36–41]. Most of the previous theoretical investigations considered the water adsorption on TiO_2 (110) in the vacuum situation. In the real photocatalytic reaction, the reactions occur in the water environment.

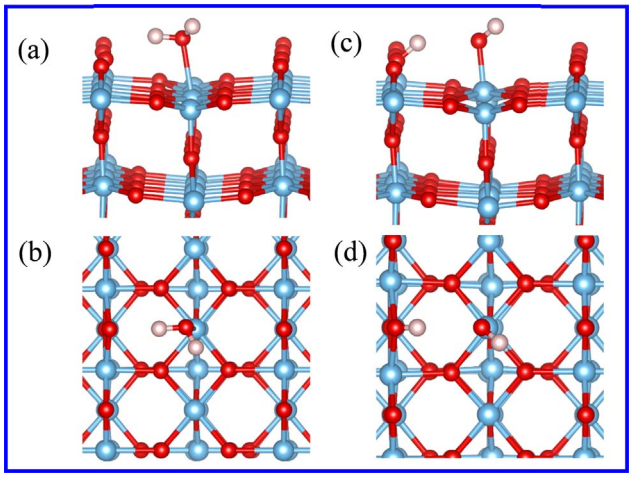

Fig. 3. The molecular and dissociated state of H_2O on rutile (110) surface. (a), (b) the side and top view of the molecular state. (c), (d) the side and top view for the dissociated state. The O atom in red, Ti atom in gray blue and H atom in pink.

In order to know the water adsorption state on the perfect TiO_2 (110) surface, we systematically study this issue by considering the solvation effect.

In this work, a (4×2) periodic rutile (110) surface was used, containing four tri-layer. And only one water molecule was adsorbed on the surface, which corresponds to 1/8 ML of water coverage. Fig. 3 shows the relaxed configurations of the molecular and dissociated states of H_2O on the rutile (110) surface. As shown in Fig. 3(a) and (b), the O atom of intact H_2O adsorbs on the top of the 5-fold coordinated Ti atom (Ti^{5c}), and one of the H atoms points to the bridge oxygen atom (O_b) and the other H atom parallels to the Ti^{5c} atom. The dissociated H_2O can be regarded as one of H atoms transfers from the water to the nearest O_b (see Fig. 3(c) and (d)).

In order to check whether water prefers to dissociate on the perfect TiO_2 (110), several different effects, such as solvation and vdW, are also considered. Table 2 displays the calculated results including the binding energy, energy difference between the molecular (M) and dissociated (D) state, and relaxed geometrical parameters for the H_2O adsorption on the perfect rutile (110). Without considering solvation effect, the PBE result shows that the binding energy is −0.66 eV for M-H_2O, which agrees with the other DFT result [39,41–43]. The energy difference is −0.24 eV, indicating that the M-H_2O is more favorable. Such results agree well with the previous works [41]. When including

Table 2
Binding energy, energy difference between the molecular and dissociated H_2O, and representative geometrical parameters for the different state H_2O adsorbed on TiO_2 surface. The letters M and D denote the molecular and dissociated state of the H_2O. The '-' and '+' mean without and with the functional, respectively. The U value is 4.2 eV. H_b is the hydrogen adsorbed on the bridge oxygen on TiO_2. The energy difference between the molecular and dissociated state of H_2O by introducing the solvation effect, which can be calculated as $\Delta E = E_M - E_D$, where E_M and E_D are the total energy for the molecular and the dissociated state of H_2O, respectively. The adsorption energy of the more stable state is bolded.

PCSM	vdW	H_2O	E_{bind} (eV)	ΔE (eV)	O-Ti^{5c} (Å)	H-O_b (Å)	O-H_b (Å)	O-H-O (θ)
−	−	**M**	**−0.66**	−0.24	2.316	2.52		107.28
		D	−0.42		1.841		2.52	
−	+	**M**	**−0.96**	−0.27	2.27	2.02		106.76
		D	−0.69		1.84		2.20	
+	−	**M**	**−1.07**	−0.29	2.273	2.39		106.24
		D	−0.78		1.804		2.58	
+	+	**M**	**−1.37**	−0.31	2.25	2.16		106.29
		D	−1.05		1.82		2.19	

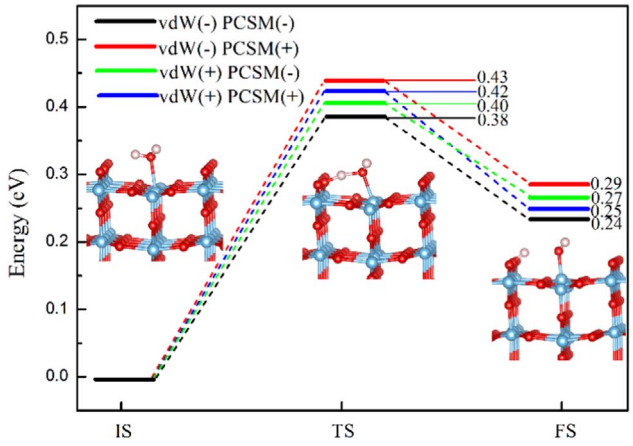

Fig. 4. Minimum energy pathway for dissociation of a H_2O molecular on a Ti^{5c} row to the O_b atom on rutile (110) surface. The sum energies of the rutile (110) and the H_2O molecular is set to the zero reference for energy.

the vdW correction, the binding energy is about 0.3 eV larger than the corresponding one for both the M- and D-H_2O calculated with PBE. The energy difference between the M- and D-H_2O is −0.27 eV, indicating the molecular state is still more stable. Recently, Sorescu *et al.* have studied the H_2O on rutile (110) surface by including the vdW correction, and the calculated binding energy is −1.01 eV for M-H_2O [44], in consistent with our result of −0.96 eV.

When the solvation effect is considered, all the calculated results are significantly changed. Firstly, the adsorption energies increase by −0.36 eV for both the M- and D-H_2O compared with the pure PBE. The energy difference between these two states increase by −0.05 eV, and the M-H_2O is still more stable. The structural behavior shows that O-Ti^{5c} distance decrease by 0.04 Å for both case, and O-H-O angle decrease by 1°.

When combination of the solvation effect with vdW correction, the binding energy increase by 0.4 eV for both the M- and D-H_2O, compared with pure vdW correction results. Similarly, the energy difference increases from −0.27 eV to −0.31 eV. The O-Ti^{5c} distance decreases by 0.02 Å for both states, while O-H-O angle decrease by 0.45°. Thus the solvation effect increases the binding energy by about 0.4 eV, and the solvation effect slightly increase the energy difference by ~0.05 eV, indicating that H_2O adsorption on the rutile (110) surface is favorable molecular state considering the solvation effect.

As shown above, the structural behavior of the H_2O is greatly affected by the solvation effect, and the water adsorption on the perfect rutile (110) prefers the intact state. It is essential to know whether the solvation effect can change the dissociated barrier of water on TiO_2 (110) in aqueous solution. In order to know this, the energy barriers are calculated with the different techniques. The calculated results are shown in Fig. 4.

Without including solvation effect, the calculated energy barrier with the pure PBE functional is 0.38 eV, which is consistent with the previous DFT result of 0.33 eV [37]. When including the vdW correction, the energy barrier becomes 0.36 eV. If solvation effect is included, reaction energy barrier with PBE functional changes from 0.38eV to 0.43 eV. If the both effects are included, the energy barrier becomes 0.42 eV. Thus when considering the solvation effect, the energy barriers of the water dissociation on the perfect TiO_2 (110) increase by 0.02–0.05 eV for the different approaches used. In all, the solvation effect can affect the reaction energy barrier in solution for the periodic semiconductor slab system.

The current PCSM model as implanted in CP2K/Quickstep has the advantage to deal with the large system compared with the others based on plane-wave DFT programs. It should be noted that the approach is not suitable for the small system size due to only single Γ point for k-point sampling implanted in CP2K/Quickstep at the current version.

4. Conclusion

In summary, we have implemented a periodic continuum solvation model that describes the effect of polarization, electrostatics, cavitation, dispersion, and pressure term in the interaction between a solute and solvent into the mixed Gaussian and plane-wave DFT code CP2K/Quickstep. The accuracy of our implanted continuum solvation model is examined for the different situations. The calculated solvation energies, configuration, and energy barrier are compared with the other available theoretical and experimental results. For non-periodic systems, the calculated solvation energies are consistent with other results within 0.17 (± 0.13) eV. Furthermore, we extent the application of our solvation model to the periodic slab systems. The results show that the solvation effect significantly changes the structure, binding energy, and the reaction energy barrier at the solid-liquid interface. The binding energy for the H_2O adsorbed on metal and semiconductor slab surface increases by about 0.4 eV when the solvation effect is considered. Meanwhile, the energy difference between the molecular and dissociated state of H_2O adsorption on the rutile TiO_2 (110) increases in solution, indicating that molecular state is more favorable in the water environments. In addition, the reaction barrier for the H_2O dissociated on rutile (110) surface increases by about 0.05 eV when the solvation effect is considered.

Acknowledgments

This work was supported by the National Natural Science Foundation of China (Nos. 51572016 and U1530401). This research is supported by a Tianhe-2JK computing time award at the Beijing Computational Science Research Center (CSRC) and the Special Program for Applied Research on Super Computation of the NSFC-Guangdong Joint Fund (the second phase).

References

[1] C.J. Cramer, D.G. Truhlar, Chem. Rev. 99 (1999) 2161.
[2] C.J. Cramer, D.G. Truhlar, Acc. Chem. Res. 41 (2008) 760.
[3] M. Zhou, X.W. Lou, Y. Xie, Nano Today 8 (2013) 598.
[4] T. Hisatomi, J. Kubota, K. Domen, Chem. Soc. Rev. 43 (2014) 7520.
[5] M.A. Henderson, Surf. Sci. 400 (1998) 203.
[6] J.A. White, E. Schwegler, G. Galli, F. Gygi, J. Chem. Phys. 113 (2000) 4668.
[7] V.B. Maurizio Cossi, Roberto Cammi, Jacopo Tomasi, Chem. Phys. Lett. 255 (1996) 327.
[8] Darrin M York, a. M. K. J., J. Phys. Chem. A 103 (1999) 11060.
[9] A.K. A.G. Schuurmann, J. Chem. Soc. 2 (1993) 799.
[10] A.W. Lange, J.M. Herbert, J. Chem. Phys. 134 (2011) 204110.
[11] L. Onsager, J. Am. Chem. Soc. 58 (1936) 1486.
[12] J.L.G. Fattebert, F, J. Comput. Chem. 23 (2002) 662.
[13] J.L. Fattebert, F. Gygi, Fr. Int. J. Quantum Chem. 93 (2003) 139.
[14] V.M. Sánchez, M. Sued, D.A. Scherlis, J. Chem. Phys. 131 (2009) 174108.
[15] D.A. Scherlis, J.L. Fattebert, F. Gygi, M. Cococcioni, N. Marzari, J. Chem. Phys. 124 (2006) 74103.
[16] D.A. Scherlis, J.L. Fattebert, N. Marzari, J. Chem. Phys. 124 (2006) 194902.
[17] V.M. Sanchez, M. Sued, D.A. Scherlis, J. Chem. Phys. 131 (2009) 174108(1).
[18] Y.-H. Fang, G.-F. Wei, Z.-P. Liu, Catal. Today 202 (2013) 98.
[19] O. Andreussi, I. Dabo, N. Marzari, J. Chem. Phys. 136 (2012) 064102(1).
[20] C. Dupont, O. Andreussi, N. Marzari, J. Chem. Phys. 139 (2013) 214110.
[21] J. VandeVondele, M. Krack, F. Mohamed, M. Parrinello, T. Chassaing, J. Hutter, Comput. Phys. Commun. 167 (2005) 103.
[22] M. Krack, Theor. Chem. Acc. 114 (2005) 145.
[23] J. Tomasi, B. Mennucci, R. Cammi, Chem. Rev. 105 (2005) 2999.
[24] J. VandeVondele, J. Hutter, J. Chem. Phys. 127 (2007) 114105.
[25] S. Goedecker, M. Teter, J. Hutter, Phys. Rev. B 54 (1996) 1703.
[26] G. Henkelman, H. Jónsson, J. Chem. Phys. 113 (2000) 9978.
[27] J.P. Perdew, K. Burke, M. Ernzerhof, Phys. Rev. Lett. 77 (1996) 3865.
[28] J. VandeVondele, J. Hutter, J. Chem. Phys. 127 (2007) 114105.
[29] Y. Sha, T.H. Yu, Y. Liu, B.V. Merinov, W.A. Goddard, J. Phys. Chem. Lett. 1 (2010) 856.
[30] F. Ya-Hui, L. Zhi-Pan, J. Phys. Chem. C 114 (2010) 4057.
[31] C.J. Cramer, D.G. Truhlar, J. Am. Chem. Soc. 113 (1991) 8305.
[32] G.D. Hawkins, C.J. Cramer, D.G. Truhlar, J. Phys. Chem. B 102 (1998) 3257.
[33] B. Ensing, E.J. Meijer, P.E. Blöchl, E.J. Baerends, J. Phys. Chem. A 105 (2001) 3300.
[34] K. Mathew, R. Sundararaman, K. Letchworth-Weaver, T.A. Arias, R.G. Hennig, J. Chem. Phys. 140 (2014) 084106.

[35] S. Meng, L. Xu, E. Wang, S. Gao, Phys. Rev. Lett. 89 (2002) 176104.
[36] Y.-F. Ji, B. Wang, Y. Luo, J. Phys. Chem. C 118 (2014) 1027.
[37] P. Lindan, C. Zhang, Phys. Rev. B 72 (2005) 075439(1).
[38] P.M. Kowalski, B. Meyer, D. Marx, Phys. Rev. B 79 (2009) 115410.
[39] L.-M. Liu, C. Zhang, G. Thornton, A. Michaelides, Phys. Rev. B 82 (2010) 161415.
[40] P.J.D. Lindan, N.M. Harrison, M.J. Gillan, Phys. Rev. Lett. 80 (1998) 762.
[41] C.-H. Sun, L.-M. Liu, A. Selloni, G.Q. Lu, S.C. Smith, J. Mater. Chem. 20 (2010) 10319.
[42] L.-M. Liu, C. Zhang, G. Thornton, A. Michaelides, Phys. Rev. B 85 (2012) 167402.
[43] L.-M. Liu, P. Crawford, P. Hu, Prog. Surf. Sci. 84 (2009) 155.
[44] D.C. Sorescu, J. Lee, W.A. Al-Saidi, K.D. Jordan, J. Chem. Phys. 137 (2012) 074704(1).